arXiv:1606.03489v2 [physics.chem-ph] 6 Aug 2016

Effect of Li Adsorption on the Electronic and Hydrogen Storage Properties of Acenes: A Dispersion-Corrected TAO-DFT Study

Sonai Seenithurai[1] and Jeng-Da Chai[1,2,*]

[1] *Department of Physics, National Taiwan University, Taipei 10617, Taiwan*

[2] *Center for Theoretical Sciences and Center for Quantum Science and Engineering, National Taiwan University, Taipei 10617, Taiwan*

(Dated: August 9, 2016)

Abstract

Due to the presence of strong static correlation effects and noncovalent interactions, accurate prediction of the electronic and hydrogen storage properties of Li-adsorbed acenes with n linearly fused benzene rings (n = 3–8) has been very challenging for conventional electronic structure methods. To meet the challenge, we study these properties using our recently developed thermally-assisted-occupation density functional theory (TAO-DFT) with dispersion corrections. In contrast to pure acenes, the binding energies of H_2 molecules on Li-adsorbed acenes are in the ideal binding energy range (about 20 to 40 kJ/mol per H_2). Besides, the H_2 gravimetric storage capacities of Li-adsorbed acenes are in the range of 9.9 to 10.7 wt%, satisfying the United States Department of Energy (USDOE) ultimate target of 7.5 wt%. On the basis of our results, Li-adsorbed acenes can be high-capacity hydrogen storage materials for reversible hydrogen uptake and release at ambient conditions.

* Author to whom correspondence should be addressed. Electronic mail: jdchai@phys.ntu.edu.tw

INTRODUCTION

Hydrogen (H_2) is a pure energy carrier with high energy content in terms of mass, and is highly abundant on the earth in the form of water. Therefore, hydrogen is considered as the next-generation clean and green fuel which could replace fossil fuels. However, the efficient production, storage, and transportation of hydrogen are to be achieved for hydrogen-based economy. Among them, the storage of hydrogen has recently posed a great challenge to the scientific community, due to the difficulty in achieving a safe and efficient storage system which could store large amounts of hydrogen in a container of small volume, light weight, and low cost [1–8].

In 2015, the United States Department of Energy (USDOE) set the 2020 target of 5.5 wt% and the ultimate target of 7.5 wt% for the gravimetric storage capacities of onboard hydrogen storage materials for light-duty vehicles [8]. As of now, there have been several methods for storing hydrogen, such as physical storage methods where hydrogen is stored in vessels at very high pressures (e.g., 350 to 700 bar), cryogenic methods where hydrogen is stored at very low temperatures (e.g., 20 K), chemical storage in the form of metal hydrides, and adsorption-based storage in high surface area materials [1–7]. Experimentally, none of these methods has achieved the gravimetric and volumetric storage capacities set by the USDOE with fast kinetics, while some theoretical studies have reported materials with the ideal storage capacities. For reversible hydrogen adsorption and desorption at ambient conditions (298 K and 1 bar), the ideal binding energies of H_2 molecules on hydrogen storage materials should be in the range of about 20 to 40 kJ/mol per H_2 [9–11].

To achieve the USDOE target, high surface area materials, such as graphene, carbon nanotubes, and metal-organic frameworks (MOFs), have been extensively studied in recent years. However, as these materials bind H_2 molecules weakly, they work properly only at low temperatures. For ambient storage applications, it is essential to increase the binding energies of H_2 molecules on these materials to the aforementioned ideal range [9–11], and hence various novel methods are being explored. Generally adopted methods are substitution doping (by B, N, etc.) and adatom adsorption (by Li, Al, Ca, Ti, etc.), just to name a few [3, 12–16]. Among them, Li adsorption is particularly attractive, because of its light weight with which a high gravimetric storage capacity could be easily achieved. In addition, as Li may adsorb H_2 molecules strongly through a charge-transfer induced polarization

mechanism [2, 17–19], the resulting hydrogen binding energy could lie in the desirable range. Consequently, a number of works have been devoted to hydrogen storage in Li-adsorbed materials [13, 15, 20–33].

Over the past two decades, organic semiconductors have received considerable attention from many researchers, owing to their potential role in molecular electronics, photonics, and photovoltaics. Among them, linear n-acenes ($C_{4n+2}H_{2n+4}$), consisting of n linearly fused benzene rings (see Figure 1(a)), have recently attracted much attention due to their unique electronic properties [34–41]. Note that n-acenes can be attractive for hydrogen storage applications, due to their quasi-one-dimensional structures and the feasibility of synthesis of shorter acenes [42, 43]. Recent interest in the development of organic field-effect transistors (OFETs) and photovoltaics has made rapid progress in acene-based crystals (e.g., tetracene, pentacene, and hexacene crystals) [44]. For example, highly oriented crystals of 6,13-bis(triisopropylsilylethynyl)pentacene (TIPS pentacene) have been experimentally realized at large scales for designing OFETs [45]. Pentacene thin films have also been synthesized, which could be hydrogen storage materials, if metal atoms can be properly intercalated as in graphite [46]. Also, because of the immense interest in the development of Li-ion battery, Li intercalation has been experimentally feasible for some carbon-based materials in recent years.

Even though there has been a keen interest in developing acene-based electronics and Li intercalation technique, the studies of electronic and hydrogen storage properties of Li-adsorbed n-acenes (see Figure 1(b)–(e)) are quite limited. Experimentally, it was argued that there is a significant decrease in the stability of longer n-acenes ($n > 5$), hindering the synthesis of these materials [42]. However, the longer acenes and acene derivatives have been synthesized in some matrices [43, 47], which also serve as the building blocks of novel MOFs and other three-dimensional crystals [11, 42, 44, 48]. Therefore, once efficient synthesis is available for the crystallization of n-acenes, Li could be subsequently intercalated to synthesize Li-adsorbed n-acenes. Theoretically, due to the multi-reference character of ground-state wavefunctions, the properties of longer n-acenes cannot be adequately described by conventional electronic structure methods, including the very popular Kohn-Sham density functional theory (KS-DFT) [49] with conventional (i.e., semilocal [50], hybrid [51–53], and double-hybrid [54–57]) density functionals [58]. High-level *ab initio* multi-reference methods are typically needed to accurately predict the properties of longer

n-acenes [34, 36, 59]. However, as the number of electrons in n-acene, $26n + 16$, quickly increases with the increase of n, there have been very scarce studies on the properties of longer n-acenes using multi-reference methods, due to their prohibitively high cost.

Recently, we have developed thermally-assisted-occupation density functional theory (TAO-DFT) [35, 38], an efficient electronic structure method for the study of large ground-state systems (e.g., containing up to a few thousand electrons) with strong static correlation effects [39–41]. Interestingly, TAO-DFT has similar computational cost as KS-DFT, and reduces to KS-DFT in the absence of strong static correlation. Very recently, we have studied the electronic properties of zigzag graphene nanoribbons (ZGNRs) using TAO-DFT, where the strong static correlation effects have been properly described [39]. Accordingly, TAO-DFT can be an ideal electronic structure method for studying the electronic properties of Li-adsorbed n-acenes. Besides, the orbital occupation numbers in TAO-DFT can be useful for examining the possible multi-reference character of Li-adsorbed n-acenes [35, 38–41]. In addition, for the hydrogen storage properties, as the interaction between H_2 and Li-adsorbed n-acenes may involve dispersion (van der Waals) interactions, electrostatic interactions, and orbital interactions [3, 10, 60], the inclusion of dispersion corrections [61, 62] in TAO-DFT can be essential to properly describe noncovalent interactions. Therefore, in this work, we adopt dispersion-corrected TAO-DFT [38] to study the electronic and hydrogen storage properties of Li-adsorbed n-acenes with various chain lengths (n = 3–8).

COMPUTATIONAL DETAILS

All calculations are performed with a development version of Q-Chem 4.3 [63]. Results are computed using TAO-BLYP-D [38] (i.e., TAO-DFT with the dispersion-corrected BLYP-D exchange-correlation density functional [61] and the LDA θ-dependent density functional E_θ^{LDA} (see Eq. (41) of Ref. [35])) at the fictitious temperature θ = 7 mhartree (as defined in Ref. [35]). For all the calculations, we adopt the 6-31G(d) basis set with the fine grid EML(75,302), consisting of 75 Euler-Maclaurin radial grid points and 302 Lebedev angular grid points. For the interaction energies of the weakly bound systems (e.g., Li binding energy, H_2 binding energy, etc.), the counterpoise correction [64] is employed to reduce the basis set superposition error (BSSE).

RESULTS AND DISCUSSION

Electronic Properties

To start with, we obtain the ground state of n-acene (n = 3–8), by performing spin-unrestricted TAO-BLYP-D calculations for the lowest singlet and triplet energies of n-acene on the respective geometries that were fully optimized at the same level of theory. The singlet-triplet energy (ST) gap of n-acene is calculated as ($E_{\mathrm{T}} - E_{\mathrm{S}}$), the energy difference between the lowest triplet (T) and singlet (S) states. Similar to previous findings [34–36, 38, 39], the ground states of n-acenes are found to be singlets for all the chain lengths investigated (see Figure 2).

Next, at the ground-state (i.e., the lowest singlet state) geometry of n-acene, we place n Li atoms on one side of n-acene, and n Li atoms on the other side (i.e., at high coverage). To obtain the most stable adsorption site, Li atoms are initially placed on different possible sites, such as the hexagon site (the center of a benzene ring), the top site (the top of a C atom), the bridge site (the midpoint of C-C bond), and the edge site (the edge of n-acene), and the structures are subsequently optimized. As illustrated in Figure 1(b), the hexagon site is the most stable adsorption site. The isolated form of Li atoms is found to be preferred over clustering [33], which may be attributed to the quasi-one-dimensional nature of n-acene. Therefore, in this work, Li-adsorbed n-acene is regarded as n-acene-2nLi, which is n-acene with $2n$ Li atoms adsorbed on all the hexagon sites.

Similar to the procedure described above, the ST gap of Li-adsorbed n-acene is also computed. As shown in Figure 2, the ST gap of Li-adsorbed n-acene generally decreases with increasing chain length. The ground states of Li-adsorbed n-acenes remain singlets for all the chain lengths studied. Owing to the presence of Li adatoms, the ST gap of Li-adsorbed n-acene is much smaller than that of pure n-acene.

Due to the symmetry constraint, the spin-restricted and spin-unrestricted energies for the lowest singlet state of pure/Li-adsorbed n-acene calculated using the exact theory, should be identical [35, 37–41]. To assess the possible symmetry-breaking effects, spin-restricted TAO-BLYP-D calculations are also performed for the lowest singlet energies on the respective optimized geometries. Within the numerical accuracy of our calculations, the spin-restricted and spin-unrestricted TAO-BLYP-D energies for the lowest singlet state of pure/Li-adsorbed

n-acene are essentially the same (i.e., essentially no unphysical symmetry-breaking effects occur in our spin-unrestricted TAO-BLYP-D calculations).

To examine the energetic stability of adsorbed Li atoms, the Li binding energy, E_b(Li), on n-acene is calculated by

$$E_b(\mathrm{Li}) = (E_{n\text{-acene}} + E_{2n\mathrm{Li}} - E_{n\text{-acene-}2n\mathrm{Li}})/2n, \tag{1}$$

where $E_{n\text{-acene}}$ is the total energy of n-acene, $E_{2n\mathrm{Li}}$ is the total energy of the $2n$ Li adatoms on the hexagon sites, and $E_{n\text{-acene-}2n\mathrm{Li}}$ is the total energy of Li-adsorbed n-acene. E_b(Li) is subsequently corrected for BSSE using a standard counterpoise correction, where the n-acene is considered as one fragment, and the $2n$ Li adatoms are considered as the other fragment. As shown in Figure 3, n-acene can strongly bind the Li adatoms with the binding energy range of 86 to 91 kJ/mol per Li.

At the ground-state (i.e., the lowest singlet state) geometry of pure/Li-adsorbed n-acene, containing N electrons, the vertical ionization potential $\mathrm{IP}_v = E_{N-1} - E_N$, vertical electron affinity $\mathrm{EA}_v = E_N - E_{N+1}$, and fundamental gap $E_g = \mathrm{IP}_v - \mathrm{EA}_v = E_{N+1} + E_{N-1} - 2E_N$ are obtained with multiple energy-difference calculations, where E_N is the total energy of the N-electron system. With increasing chain length, IP_v monotonically decreases (see Figure 4), EA_v monotonically increases (see Figure 5), and hence E_g monotonically decreases (see Figure 6). As shown, the IP_v, EA_v, and E_g values of Li-adsorbed n-acene are less sensitive to the chain length than those of pure n-acene. Note also that the E_g value of Li-adsorbed n-acene (n = 4–8) is within the most interesting range (1 to 3 eV), giving promise for applications of Li-adsorbed n-acenes in nanophotonics.

To assess the possible multi-reference character of pure/Li-adsorbed n-acene, we calculate the symmetrized von Neumann entropy [37–39, 41]

$$S_{\mathrm{vN}} = -\frac{1}{2}\sum_{i=1}^{\infty}\Big\{f_i\,\ln(f_i) + (1-f_i)\,\ln(1-f_i)\Big\} \tag{2}$$

for the lowest singlet state of pure/Li-adsorbed n-acene as a function of the chain length. Here, f_i the occupation number of the i^{th} orbital obtained with TAO-BLYP-D, ranging from 0 to 1, is approximately equal to the occupation number of the i^{th} natural orbital [35, 38]. Note that S_{vN} provides insignificant contributions for a single-reference system ($\{f_i\}$ are close to either 0 or 1), and rapidly increases with the number of active orbitals ($\{f_i\}$ are fractional for active orbitals, and are close to either 0 or 1 for others). As shown in Figure 7,

S_{vN} monotonically increases with the chain length. Therefore, the multi-reference character of pure/Li-adsorbed n-acene increases with the chain length.

On the basis of several measures (e.g., the smaller ST gap, the smaller E_g, and the larger S_{vN}), Li-adsorbed n-acene should possess stronger multi-reference character than pure n-acene for each n. Consequently, KS-DFT with conventional density functionals should be insufficient for the accurate description of the properties of Li-adsorbed n-acene. Besides, as accurate multi-reference calculations are prohibitively expensive for the longer pure/Li-adsorbed n-acene, the use of TAO-DFT in this study is well justified.

Hydrogen Storage Properties

As pure carbon-based materials bind H_2 molecules weakly (i.e., mainly governed by dispersion interactions), they are not ideal hydrogen storage materials at ambient conditions [9]. Similarly, pure n-acenes are not promising for ambient storage applications, as the binding energies of H_2 molecules remain small. Besides, the number of H_2 molecules that can be adsorbed on each benzene ring is limited, due to the repulsive interaction between the adsorbed H_2 molecules at short distances [65]. Therefore, the more the adsorbed H_2 molecules, the less the average H_2 binding energy on n-acene. Consequently, pure n-acenes cannot be high-capacity hydrogen storage materials at ambient conditions.

Here, we examine the hydrogen storage properties of Li-adsorbed n-acene (n = 3–8). As illustrated in Figure 1, at the ground-state geometry of Li-adsorbed n-acene, x H_2 molecules (x = 1–3) are initially placed on different possible sites around each Li adatom, and the structures are subsequently optimized to obtain the most stable geometry. All the H_2 molecules are found to be adsorbed molecularly. The average H_2 binding energy, $E_b(H_2)$, on Li-adsorbed n-acene is calculated by

$$E_b(\mathrm{H_2}) = (E_{n\text{-acene-}2n\mathrm{Li}} + 2nxE_{\mathrm{H_2}} - E_{n\text{-acene-}2n\mathrm{Li}\text{-}2nx\mathrm{H_2}})/(2nx). \quad (3)$$

Here, $E_{\mathrm{H_2}}$ is the total energy of a free H_2 molecule, and $E_{n\text{-acene-}2n\mathrm{Li}\text{-}2nx\mathrm{H_2}}$ is the total energy of Li-adsorbed n-acene with x H_2 molecules adsorbed on each Li adatom. $E_b(H_2)$ is subsequently corrected for BSSE using a standard counterpoise correction. As shown in Figure 8, $E_b(H_2)$ is in the range of 31 to 43 kJ/mol per H_2 for x = 1, in the range of 30 to 32 kJ/mol per H_2 for x = 2, and in the range of 21 to 22 kJ/mol per H_2 for x = 3, falling in the ideal

binding energy range.

Here, we examine if the binding energies of successive H_2 molecules are in the ideal binding energy range (i.e., not just the average H_2 binding energy). The binding energy of the y^{th} H_2 molecule (y = 1–3), $E_{b,y}(H_2)$, on Li-adsorbed n-acene is calculated by

$$E_{b,y}(H_2) = (E_{n\text{-acene-}2n\text{Li-}2n(y-1)H_2} + 2nE_{H_2} - E_{n\text{-acene-}2n\text{Li-}2nyH_2})/(2n). \quad (4)$$

Similarly, $E_{b,y}(H_2)$ is subsequently corrected for BSSE using a standard counterpoise correction. As shown in Figure 9, $E_{b,1}(H_2)$ is in the range of 31 to 43 kJ/mol per H_2, $E_{b,2}(H_2)$ is in the range of 20 to 29 kJ/mol per H_2, and $E_{b,3}(H_2)$ is about 3 kJ/mol per H_2. Therefore, while the first and second H_2 molecules can be adsorbed on Li-adsorbed n-acene in the ideal binding energy range, the third H_2 molecule is only weakly adsorbed (i.e., not suitable for ambient temperature storage).

For practical applications, we estimate the desorption temperature, T_D, of the adsorbed H_2 molecules using the van't Hoff equation [12, 15],

$$T_D = \frac{E_b(H_2)}{k_B}\left\{\frac{\Delta S}{R} - \ln\frac{p_0}{p_{eq}}\right\}^{-1}. \quad (5)$$

Here, $E_b(H_2)$ is the average H_2 binding energy (see Eq. (3)), ΔS is the change in hydrogen entropy from gas to liquid phase ($\Delta S = 13.819R$ taken from Ref. [66]), p_0 is the standard atmospheric pressure (1 bar), p_{eq} is the equilibrium pressure, k_B is the Boltzmann constant, and R is the gas constant. As shown in Table I, T_D for Li-adsorbed n-acene (n = 3–8) with x H_2 molecules (x = 1–2) adsorbed on each Li adatom, is estimated using Eq. (5) at p_{eq} = 1.5 bar (as adopted in Ref. [9]) and at p_{eq} = 1 bar (the standard atmospheric pressure). For Li-adsorbed n-acene (except for n = 3), the T_D values are slightly higher than room temperature for x = 1, and slightly lower than room temperature for x = 2. Even for Li-adsorbed 3-acene, the T_D values remain close to room temperature. Therefore, Li-adsorbed n-acenes can be viable hydrogen storage materials at ambient conditions.

As Li-adsorbed n-acene (n = 3–8) can bind up to $4n$ H_2 molecules (i.e., each Li adatom can bind up to two H_2 molecules) with the average and successive H_2 binding energies in the ideal range, the corresponding H_2 gravimetric storage capacity, C_g, is evaluated by

$$C_g = \frac{4nM_{H_2}}{M_{n\text{-acene-}2n\text{Li}} + 4nM_{H_2}}, \quad (6)$$

where $M_{n\text{-acene-}2n\text{Li}}$ is the mass of Li-adsorbed n-acene, and M_{H_2} is the mass of H_2. As shown in Table I, C_g is in the range of 9.9 to 10.7 wt%, satisfying the USDOE ultimate

target of 7.5 wt%. Based on the observed trends, at the polymer limit ($n \to \infty$), the C_g value of Li-adsorbed polyacene can be estimated as 11.2 wt%, very close to that of Li-adsorbed n-acene (n = 3–8). However, the USDOE target value refers to the complete storage system, including the storage material, enclosing tank, insulation, piping, etc. [8], rather than the storage material alone. Therefore, the C_g values obtained here may not be directly compared to the USDOE target. The real C_g value will depend on the design of the complete storage system, and hence the comparison has to be made after considering all of these issues. Nonetheless, as the C_g values obtained here are much higher than the USDOE ultimate target, the complete storage systems based on Li-adsorbed n-acenes are likely to be high-capacity hydrogen storage materials at ambient conditions.

CONCLUSIONS

In conclusion, we have studied the electronic properties (i.e., the Li binding energies, ST gaps, vertical ionization potentials, vertical electron affinities, fundamental gaps, and symmetrized von Neumann entropy) and hydrogen storage properties (i.e., the average and successive H_2 binding energies, H_2 desorption temperatures, and H_2 gravimetric storage capacities) of Li-adsorbed n-acenes (n = 3–8) using our recently developed TAO-DFT with dispersion corrections. Since Li-adsorbed n-acenes have been shown to exhibit stronger multi-reference character than pure n-acenes, KS-DFT with conventional density functionals can be unreliable for studying the properties of these systems. Besides, accurate multi-reference calculations are prohibitively expensive for the longer Li-adsorbed n-acenes, and hence the use of TAO-DFT in this study is well justified. On the basis of our results, Li-adsorbed n-acenes can bind up to $4n$ H_2 molecules (i.e., each Li adatom can bind up to two H_2 molecules) with the average and successive H_2 binding energies in the ideal range of about 20 to 40 kJ/mol per H_2. Consequently, for Li-adsorbed n-acenes, the H_2 desorption temperatures are close to room temperature, and the H_2 gravimetric storage capacities are in the range of 9.9 to 10.7 wt%, satisfying the USDOE ultimate target of 7.5 wt%. Therefore, Li-adsorbed n-acenes could serve as high-capacity hydrogen storage materials for reversible hydrogen uptake and release at ambient conditions.

On the basis of our results, it is possible to place Li on both sides of the acene molecule. However, for acene crystals (i.e., real materials), it can be challenging to place Li on both

side of the acene molecule, as the acene molecules are stacked against each other. To resolve this, we may follow the proposal of Deng *et al.* [21], and consider Li-adsorbed pillared acenes, where the intermolecular distance of acene molecules can be properly increased to provide sufficiently large space for Li and H_2. A systematic study of the electronic and hydrogen storage properties of Li-adsorbed pillared acenes is essential, and may be considered for future work. In addition, it should be noted that Li-doped systems could have the following practical issues: the preoccupancy of Li sites by solvent molecules, low stability against air and water, etc., which are open to experimentalists [33].

We hope that our results will guide experimental studies for developing and synthesizing reversible hydrogen storage materials. Owing to recent advances in dispersion-corrected TAO-DFT, the search for ideal hydrogen storage materials can be readily extended to large systems with strong static correlation effects (i.e., systems beyond the reach of conventional electronic structure methods). In the future, we intend to address how the electronic and hydrogen storage properties vary with different adatoms (e.g., Al, Ca, Ti, etc.) and underlying carbon-based materials (e.g., graphene nanoribbons, nanoflakes, etc.).

ACKNOWLEDGEMENTS

This work was supported by the Ministry of Science and Technology of Taiwan (Grant No. MOST104-2628-M-002-011-MY3), National Taiwan University (Grant No. NTU-CDP-105R7818), the Center for Quantum Science and Engineering at NTU (Subproject Nos.: NTU-ERP-105R891401 and NTU-ERP-105R891403), and the National Center for Theoretical Sciences of Taiwan.

AUTHOR CONTRIBUTIONS

S.S. and J.-D.C. designed the project. S.S. performed the calculations. S.S. and J.-D.C. contributed to the data analysis and writing of the paper.

ADDITIONAL INFORMATION

Competing financial interests: The authors declare no competing financial interests.

---

[1] Schlapbach, L. & Züttel, A. Hydrogen-storage materials for mobile applications. *Nature* **414**, 353–358 (2001).

[2] Jena, P. Materials for hydrogen storage: past, present, and future. *J. Phys. Chem. Lett.* **2**, 206–211 (2011).

[3] Park, N. *et al.* Progress on first-principles-based materials design for hydrogen storage. *PNAS* **109**, 19893–19899 (2012).

[4] Dalebrook, A. F., Gan, W., Grasemann, M., Moret, S. & Laurenczy, G. Hydrogen storage: beyond conventional methods. *Chem. Commun.* **49**, 8735–8751 (2013).

[5] Durbin, D. & Malardier-Jugroot, C. Review of hydrogen storage techniques for on board vehicle applications. *Int. J. Hydrogen Energy* **38**, 14595–14617 (2013).

[6] Tozzini, V. & Pellegrini, V. Prospects for hydrogen storage in graphene. *Phys. Chem. Chem. Phys.* **15**, 80–89 (2013).

[7] Das, G. & Bhattacharya, S. Simulation, modelling and design of hydrogen storage materials. *Proc. Indian. Nat. Sci. Acad.* **81**, 939–951 (2015).

[8] U. S. Department of Energy., *Target explanation document: onboard hydrogen storage for light-duty fuel cell vehicles. Technical report.* (2015) Available at: `http://energy.gov/eere/fuelcells/hydrogen-storage` (accessed: June 2016).

[9] Bhatia, S. K. & Myers, A. L. Optimum conditions for adsorptive storage. *Langmuir* **22**, 1688–1700 (2006).

[10] Lochan, R. C. & Head-Gordon, M. Computational studies of molecular hydrogen binding affinities: the role of dispersion forces, electrostatics, and orbital interactions. *Phys. Chem. Chem. Phys.* **8**, 1357–1370 (2006).

[11] Sumida, K. *et al.* Impact of metal and anion substitutions on the hydrogen storage properties of M-BTT metal-organic frameworks. *J. Am. Chem. Soc.* **135**, 1083–1091 (2013).

[12] Durgun, E., Ciraci, S. & Yildirim, T. Functionalization of carbon-based nanostructures with light transition-metal atoms for hydrogen storage. *Phys. Rev. B* **77**, 085405 (2008).

[13] Seenithurai, S., Pandyan, R. K., Vinodh Kumar, S., Saranya, C. & Mahendran, M. Li-decorated double vacancy graphene for hydrogen storage application: a first principles study. *Int. J. Hydrogen Energy* **39**, 11016–11026 (2014).

[14] Seenithurai, S., Pandyan, R. K., Vinodh Kumar, S., Saranya, C. & Mahendran, M. Al-decorated carbon nanotube as the molecular hydrogen storage medium. *Int. J. Hydrogen Energy* **39**, 11990–11998 (2014).

[15] Qiu, N.-X., Zhang, C.-H. & Xue, Y. Tuning hydrogen storage in lithium-functionalized BC_2N sheets by doping with boron and carbon. *ChemPhysChem* **15**, 3015–3025 (2014).

[16] Lebon, A., Carrete, J., Gallego, L. & Vega, A. Ti-decorated zigzag graphene nanoribbons for hydrogen storage. A van der Waals-corrected density-functional study. *Int. J. Hydrogen Energy* **40**, 4960–4968 (2015).

[17] Niu, J., Rao, B. K. & Jena, P. Binding of hydrogen molecules by a transition-metal ion. *Phys. Rev. Lett.* **68**, 2277–2280 (1992).

[18] Niu, J., Rao, B. K., Jena, P. & Manninen, M. Interaction of H_2 and He with metal atoms, clusters, and ions. *Phys. Rev. B* **51**, 4475–4484 (1995).

[19] Froudakis, G. E. Why alkali-metal-doped carbon nanotubes possess high hydrogen uptake. *Nano Lett.* **1**, 531–533 (2001).

[20] Chen, P., Wu, X., Lin, J. & Tan, K. L. High H_2 uptake by alkali-doped carbon nanotubes under ambient pressure and moderate temperatures. *Science* **285**, 91–93 (1999).

[21] Deng, W.-Q., Xu, X. & Goddard, W. A. New alkali doped pillared carbon materials designed to achieve practical reversible hydrogen storage for transportation. *Phys. Rev. Lett.* **92**, 166103 (2004).

[22] Sun, Q., Jena, P., Wang, Q. & Marquez, M. First-principles study of hydrogen storage on $Li_{12}C_{60}$. *J. Am. Chem. Soc.* **128**, 9741–9745 (2006).

[23] Sabir, A. K., Lu, W., Roland, C. & Bernholc, J. Ab initio simulations of H_2 in Li-doped carbon nanotube systems. *J. Phys.: Condens. Matter* **19**, 086226 (2007).

[24] Li, Y., Zhou, G., Li, J., Gu, B.-L. & Duan, W. Alkali-metal-doped B_{80} as high-capacity hydrogen storage media. *J. Phys. Chem. C* **112**, 19268–19271 (2008).

[25] Er, S., de Wijs, G. A. & Brocks, G. Hydrogen storage by polylithiated molecules and nanostructures. *J. Phys. Chem. C* **113**, 8997–9002 (2009).

[26] Hussain, T. *et al.* Ab initio study of lithium-doped graphane for hydrogen storage. *EPL* **96**, 27013 (2011).

[27] Huang, S.-H. *et al.* Lithium-decorated oxidized porous graphene for hydrogen storage by first principles study. *J. Appl. Phys.* **112**, 124312 (2012).

[28] Wang, Q. & Jena, P. Density functional theory study of the interaction of hydrogen with Li_6C_{60}. *J. Phys. Chem. Lett.* **3**, 1084–1088 (2012).

[29] Li, P., Deng, S., Zhang, L., Liu, G. H. & Yu, J. Hydrogen storage in lithium-decorated benzene complexes. *Int. J. Hydrogen Energy* **37**, 17153–17157 (2012).

[30] Kolmann, S. J., D'Arcy, J. H. & Jordan, M. J. T. Quantum effects and anharmonicity in the H_2-Li^+-benzene complex: a model for hydrogen storage materials. *J. Chem. Phys.* **139**, 234305 (2013).

[31] Hu, Z.-Y, Shao, X., Wang, D., Liu, L.-M & Johnson, J. K. A first-principles study of lithium-decorated hybrid boron nitride and graphene domains for hydrogen storage. *J. Chem. Phys.* **141**, 084711 (2014).

[32] Gaboardi, M. *et al.* In situ neutron powder diffraction of Li_6C_{60} for hydrogen storage. *J. Phys. Chem. C* **119**, 19715–19721 (2015).

[33] Xu, D., Sun, L., Li, G., Shang, J., Yang, R.-X. & Deng, W.-Q. Methyllithium-doped naphthyl-containing conjugated microporous polymer with enhanced hydrogen storage performance. *Chem. Eur. J.* **22**, 7944–7949 (2016).

[34] Hachmann, J., Dorando, J. J., Aviles, M. & Chan, G. K. L. The radical character of the acenes: a density matrix renormalization group study. *J. Chem. Phys.* **127**, 134309 (2007).

[35] Chai, J.-D. Density functional theory with fractional orbital occupations. *J. Chem. Phys.* **136**, 154104 (2012).

[36] Mizukami, W., Kurashige, Y. & Yanai, T. More π electrons make a difference: emergence of many radicals on graphene nanoribbons studied by ab initio DMRG theory. *J. Chem. Theory and Comput.* **9**, 401–407 (2013).

[37] Rivero, P., Jiménez-Hoyos, C. A. & Scuseria, G. E. Entanglement and polyradical character of polycyclic aromatic hydrocarbons predicted by projected Hartree-Fock theory. *J. Phys. Chem. B* **117**, 12750–12758 (2013).

[38] Chai, J.-D. Thermally-assisted-occupation density functional theory with generalized-gradient approximations. *J. Chem. Phys.* **140**, 18A521 (2014).

[39] Wu, C.-S. & Chai, J.-D. Electronic properties of zigzag graphene nanoribbons studied by TAO-DFT. *J. Chem. Theory Comput.* **11**, 2003–2011 (2015).

[40] Yeh, C.-N. & Chai, J.-D. Role of Kekulé and non-Kekulé structures in the radical character of alternant polycyclic aromatic hydrocarbons: a TAO-DFT study. *Sci. Rep.* **6**, 30562 (2016).

[41] Wu, C.-S., Lee, P.-Y. & Chai, J.-D. Electronic properties of cyclacenes from TAO-DFT. e-print arXiv:1607.04900.

[42] Ye, Q. & Chi, C. Recent highlights and perspectives on acene based molecules and materials. *Chem. Mater.* **26**, 4046–4056 (2014).

[43] Bettinger, H. F. & Tönshoff, C. The longest acenes. *Chem. Rec.* **15**, 364–369 (2015).

[44] Morisaki, H. *et al.* Large surface relaxation in the organic semiconductor tetracene. *Nat. Commun.* **5**, 5400 (2014).

[45] Zhao, H., Wang, Z., Dong, G. & Duan, L. Fabrication of highly oriented large-scale TIPS pentacene crystals and transistors by the Marangoni effect-controlled growth method. *Phys. Chem. Chem. Phys.* **17**, 6274–6279 (2015).

[46] Nabok, D. *et al.* Crystal and electronic structures of pentacene thin films from grazing-incidence x-ray diffraction and first-principles calculations. *Phys. Rev. B* **76**, 235322 (2007).

[47] Zade, S. S. & Bendikov, M. Heptacene and beyond: the longest characterized acenes. *Angew. Chem. Int. Ed.* **49**, 4012–4015 (2010).

[48] Desiraju, G. R. Crystal engineering: from molecule to crystal. *J. Am. Chem. Soc.* **135**, 9952–9967 (2013).

[49] Kohn, W. & Sham, L. J. Self-consistent equations including exchange and correlation effects. *Phys. Rev.* **140**, A1133–A1138 (1965).

[50] Perdew, J. P., Burke, K. & Ernzerhof, M. Generalized gradient approximation made simple. *Phys. Rev. Lett.* **77**, 3865–3868 (1996).

[51] Becke, A. D. density-functional thermochemistry. III. The role of exact exchange. *J. Chem. Phys.* **98**, 5648–5652 (1993).

[52] Lin, Y.-S., Tsai, C.-W., Li, G.-D. & Chai, J.-D. Long-range corrected hybrid meta-generalized-gradient approximations with dispersion corrections. *J. Chem. Phys.* **136**, 154109 (2012).

[53] Lin, Y.-S., Li, G.-D., Mao, S.-P. & Chai, J.-D. Long-range corrected hybrid density functionals with improved dispersion corrections. *J. Chem. Theory Comput.* **9**, 263–272 (2013).

[54] Grimme, S. Semiempirical hybrid density functional with perturbative second-order correlation. *J. Chem. Phys.* **124**, 034108 (2006).

[55] Chai, J.-D. & Head-Gordon, M. Long-range corrected double-hybrid density functionals. *J. Chem. Phys.* **131**, 174105 (2009).

[56] Chai, J.-D. & Mao, S.-P. Seeking for reliable double-hybrid density functionals without fitting parameters: the PBE0-2 functional. *Chem. Phys. Lett.* **538**, 121–125 (2012).

[57] Hui, K. & Chai, J.-D. SCAN-based hybrid and double-hybrid density functionals from models without fitted parameters. *J. Chem. Phys.* **144**, 044114 (2016).

[58] Cohen, A. J., Mori-Sánchez, P. & Yang, W. Challenges for density functional theory. *Chem. Rev.* **112**, 289–320 (2012).

[59] Gryn'ova, G., Coote, M. L. & Corminboeuf, C. Theory and practice of uncommon molecular electronic configurations. *WIREs Comput. Mol. Sci.* **5**, 440–459 (2015).

[60] Tsivion, E., Long, J. R. & Head-Gordon, M. Hydrogen physisorption on metal-organic framework linkers and metalated linkers: a computational study of the factors that control binding strength. *J. Am. Chem. Soc.* **136**, 17827–17835 (2014).

[61] Grimme, S. Semiempirical GGA-type density functional constructed with a long-range dispersion correction. *J. Comput. Chem.* **27**, 1787–1799 (2006).

[62] Grimme, S., Hansen, A., Brandenburg, J. G. & Bannwarth, C. Dispersion-corrected mean-field electronic structure methods. *Chem. Rev.* **116**, 5105–5154 (2016).

[63] Shao, Y. *et al.* Advances in molecular quantum chemistry contained in the Q-Chem 4 program package. *Mol. Phys.* **113**, 184–215 (2015).

[64] Boys, S. F. & Bernardi, F. The calculation of small molecular interactions by the differences of separate total energies. Some procedures with reduced errors. *Mol. Phys.* **19**, 553–566 (1970).

[65] Okamoto, Y. & Miyamoto, Y. Ab initio investigation of physisorption of molecular hydrogen on planar and curved graphenes. *J. Phys. Chem. B* **105**, 3470–3474 (2001).

[66] Lemmon, E. W. in *Handbook of Chemistry and Physics 96th edn* (eds Haynes, W. M. *et al.*) Section 6, 21–37 (CRC Press, 2016)

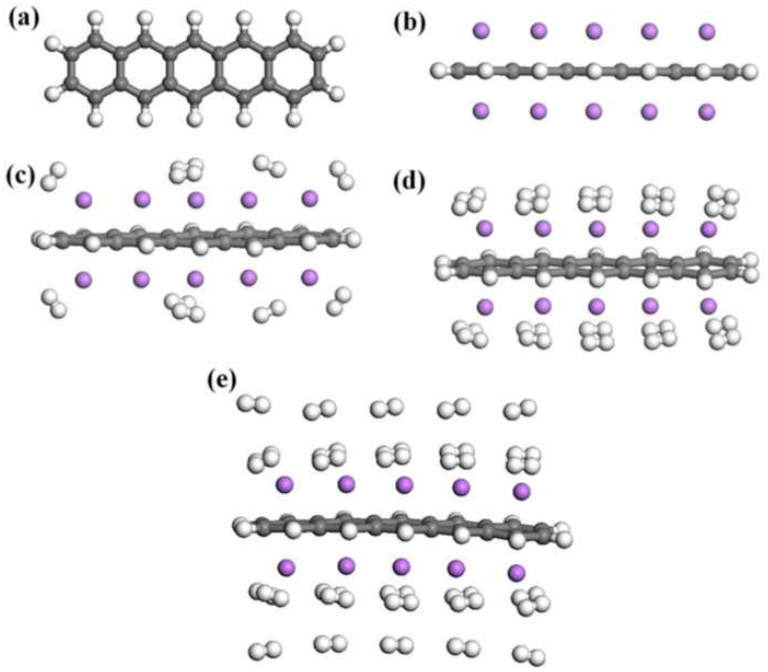

FIG. 1. Structures of (a) pure 5-acene, (b) Li-adsorbed 5-acene, (c) Li-adsorbed 5-acene with one H_2 molecule adsorbed on each Li adatom, (d) Li-adsorbed 5-acene with two H_2 molecules adsorbed on each Li adatom, and (e) Li-adsorbed 5-acene with three H_2 molecules adsorbed on each Li adatom. Here, grey, white, and purple balls represent C, H, and Li atoms, respectively.

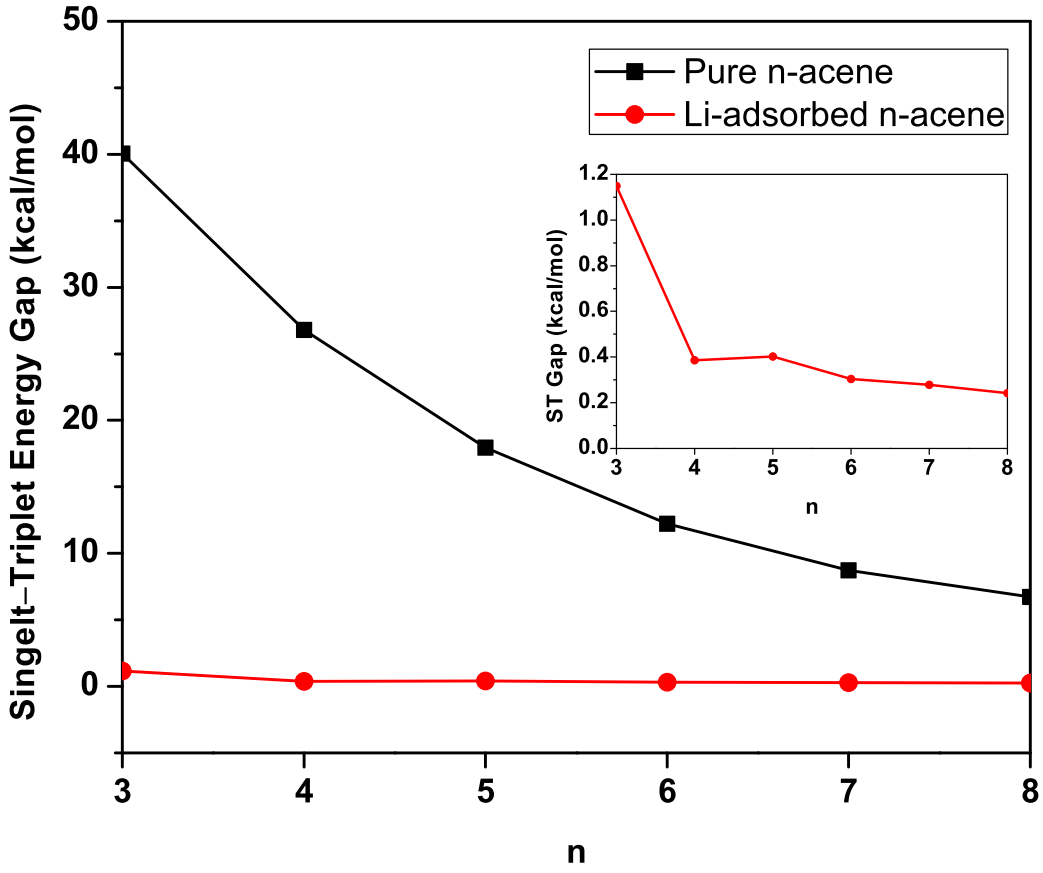

FIG. 2. Singlet-triplet energy (ST) gap of pure/Li-adsorbed n-acene as a function of the chain length, calculated using TAO-BLYP-D. The inset shows a close-up view for the ST gap of Li-adsorbed n-acene.

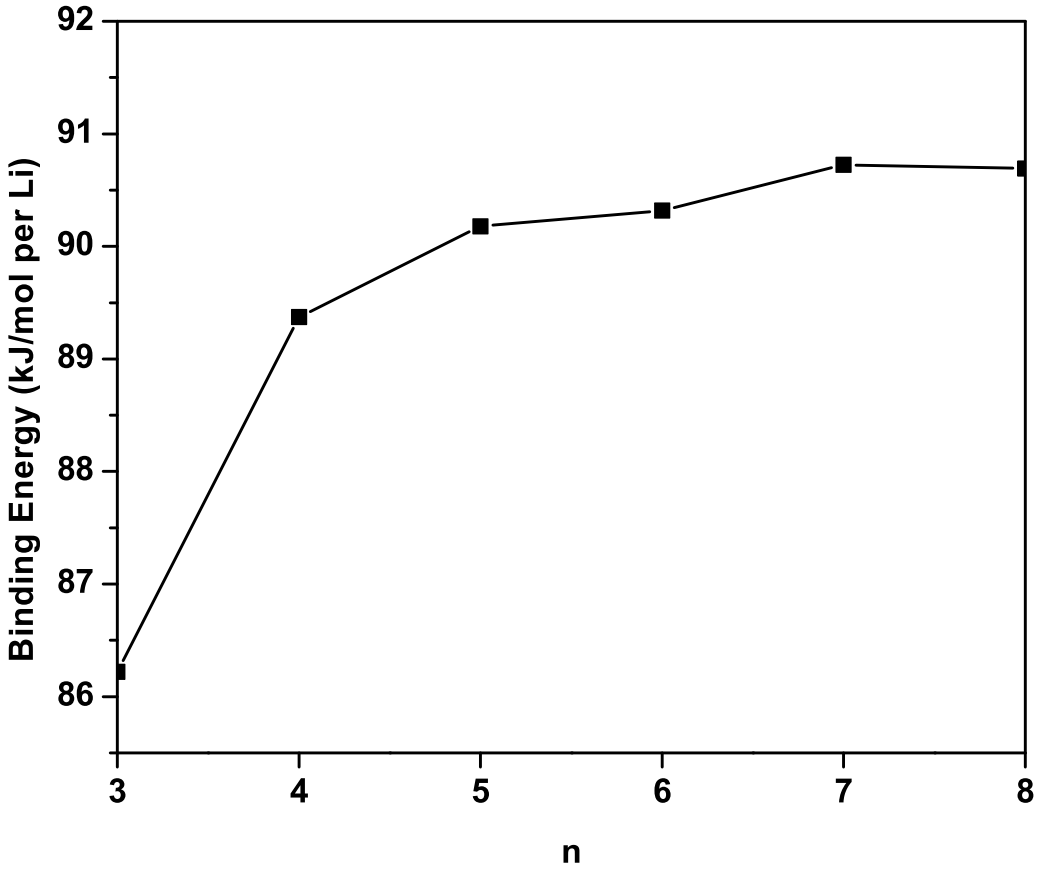

FIG. 3. Li binding energy on n-acene as a function of the chain length, calculated using TAO-BLYP-D.

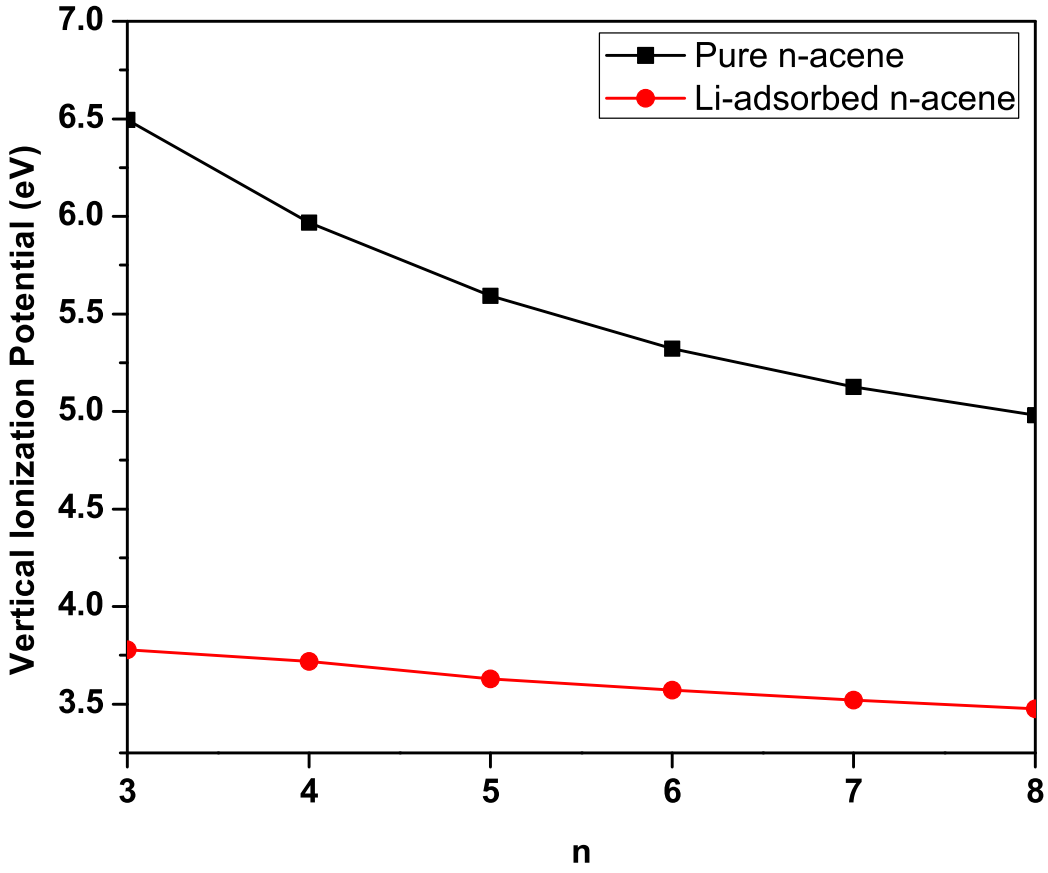

FIG. 4. Vertical ionization potential for the lowest singlet state of pure/Li-adsorbed n-acene as a function of the chain length, calculated using TAO-BLYP-D.

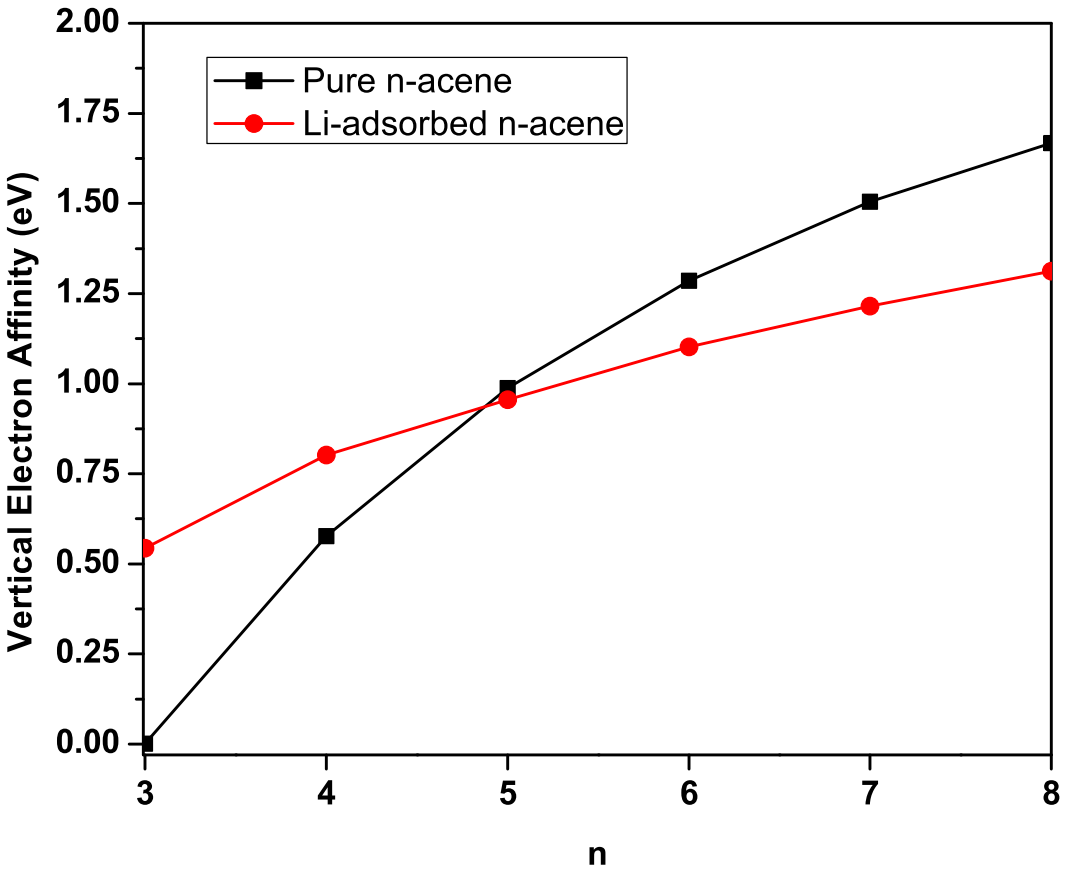

FIG. 5. Vertical electron affinity for the lowest singlet state of pure/Li-adsorbed n-acene as a function of the chain length, calculated using TAO-BLYP-D.

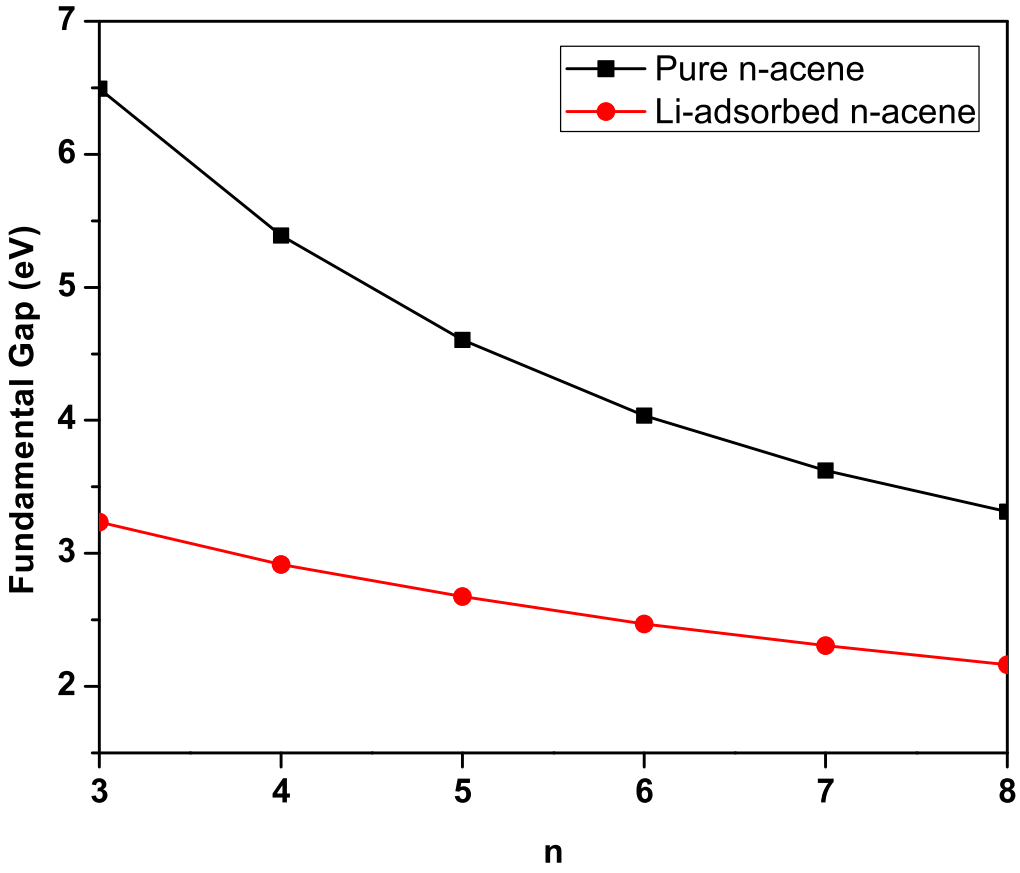

FIG. 6. Fundamental gap for the lowest singlet state of pure/Li-adsorbed n-acene as a function of the chain length, calculated using TAO-BLYP-D.

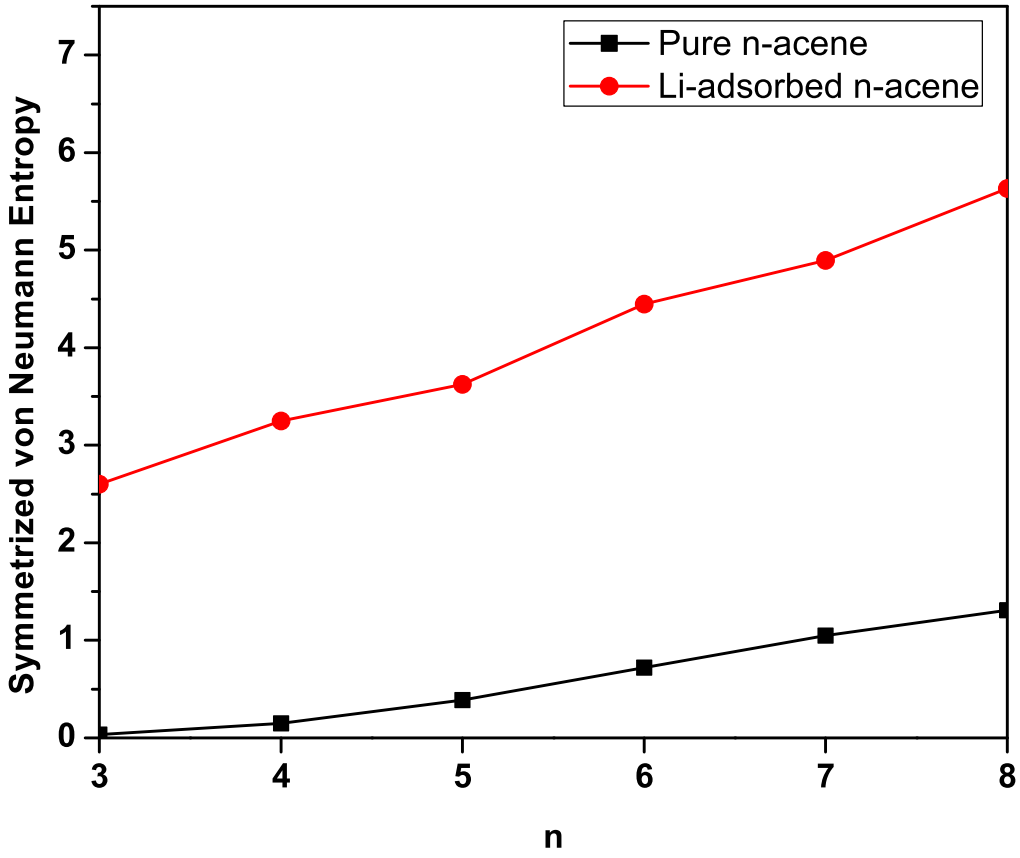

FIG. 7. Symmetrized von Neumann entropy for the lowest singlet state of pure/Li-adsorbed n-acene as a function of the chain length, calculated using TAO-BLYP-D.

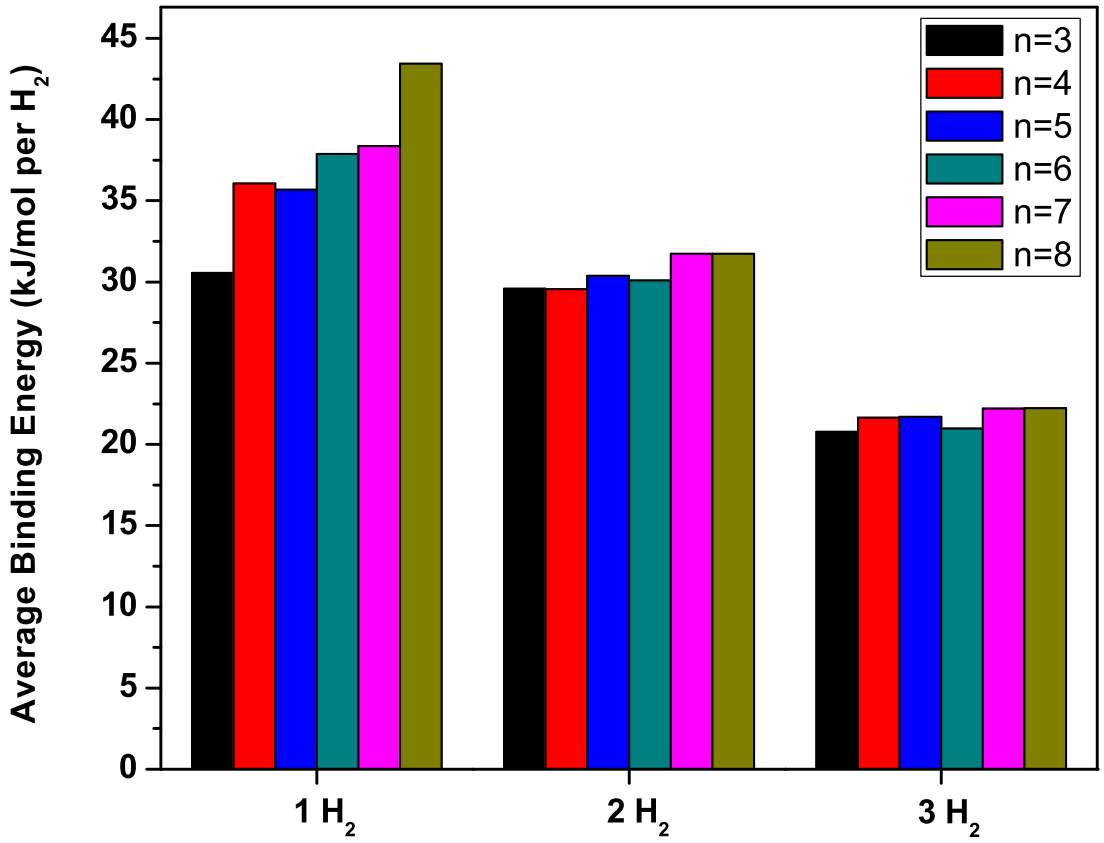

FIG. 8. Average H_2 binding energy on Li-adsorbed n-acene ($n = 3$–8) as a function of the number of H_2 molecules adsorbed on each Li adatom, calculated using TAO-BLYP-D.

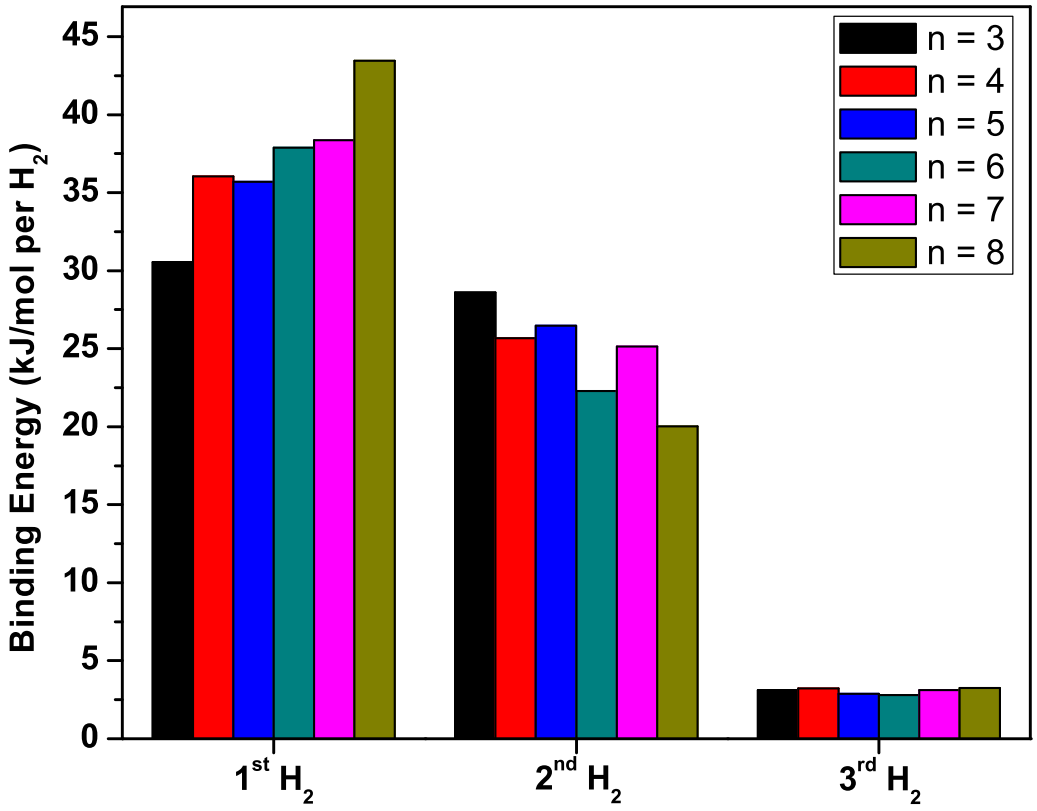

FIG. 9. Binding energy of the y^{th} H_2 molecule (y = 1–3) on Li-adsorbed n-acene (n = 3–8), calculated using TAO-BLYP-D.

TABLE I. Average H_2 binding energy $E_b(H_2)$ (kJ/mol per H_2), H_2 desorption temperature T_D (K), and H_2 gravimetric storage capacity C_g (wt%) for Li-adsorbed n-acene (n = 3–8) with x H_2 molecules (x = 1–2) adsorbed on each Li adatom, calculated using TAO-BLYP-D. Here, T_D is estimated using the van't Hoff equation (see Eq. (5)) at $p_{eq} = 1.5$ (bar) and at $p_{eq} = 1$ (bar), and C_g (see Eq. (6)) is calculated only for $x = 2$.

n	$E_b(H_2)$		T_D ($p_{eq} = 1.5$)		T_D ($p_{eq} = 1$)		C_g
	1 H_2	2 H_2	1 H_2	2 H_2	1 H_2	2 H_2	
3	30.55	29.58	258	250	266	258	9.9
4	36.06	30.87	305	261	314	269	10.2
5	35.69	31.08	302	263	311	270	10.4
6	37.87	30.08	320	254	330	262	10.5
7	38.36	31.75	324	269	334	276	10.6
8	43.45	31.73	368	268	378	276	10.7